Astron. Astrophys. 344, 1–6 (1999)

ASTRONOMY AND ASTROPHYSICS

Scaling analysis of galaxy distribution in the CfA2 data

Tomomi Kurokawa[1], **Masahiro Morikawa**[1], **and Hideaki Mouri**[2]

[1] Department of Physics, Ochanomizu University, 2-2-1 Otsuka, Bunkyo, Tokyo 112-0012, Japan
[2] Meteorological Research Institute, 1-1 Nagamine, Tsukuba 305-0052, Japan

Received 21 October 1998 / Accepted 4 January 1999

Abstract. The southern CfA2 galaxy data are used to investigate the scaling properties of the galaxy number distribution. We construct two volume-limited samples with galaxy magnitudes $M_{B(0)} \leq -19.42$ and $M_{B(0)} \leq -20.00$, and calculate the second- to ninth-order moments with the box-counting method. On scales from 5 to 27 h^{-1} Mpc, the moments exhibit multifractal scalings. From the exponents of the scalings, we suggest that the galaxies lie in planar structures which have filamentary dense regions.

Key words: methods: statistical – cosmology: large-scale structure of Universe

1. Introduction

During the last two decades, redshift surveys have revealed that the galaxy distribution has structures on various scales, $i.e.$, clusters, filaments, sheets, voids, and so on ($e.g.$, Geller & Huchra 1989). To quantify the complex appearance of those structures, and also to test models for the evolution of those structures, statistical characterization of them is required. The most standard statistical tool is the two-point correlation function ($e.g.$, Davis & Peebles 1983). However, the two-point correlation is merely equivalent to the second-order moment of the distribution. If the galaxy distribution is to be discussed in more detail, the higher-order moments are required. This situation calls for a new "multifractal" approach, which consists in characterizing the scaling properties of moments at all the orders (Parisi & Frisch 1985; Jensen et al. 1985; Halsey et al. 1986; see also Sect. 2).

We undertake a multifractal analysis of the galaxy number density. Though such analyses have been carried out so far ($e.g.$, Jones et al. 1988; Coleman & Pietronero 1992; Domínguez-Tenreiro et al. 1994; Martínez & Coles 1994; Ueda 1995), we try to make our present analysis more reliable than those in previous works. First, the data to be used are from the CfA2 survey (Huchra et al. 1999). This survey is complete to $m_{B(0)} = 15.5$ and covers a wide area of the sky. Since the volume of the CfA2 sample is quite large, we do not have to make any assumption on the volume boundaries (Sect. 3). Second, the statistical confidence of our analysis is examined with artificial samples (Sect. 4). This kind of examination is important, since any galaxy sample is composed of a finite number of discrete data (Dubrulle & Lachièze-Rey 1994). Consequently, it is established that the galaxy distribution is multifractal in a range of the scales (Sect. 5). We discuss some structural implications of our result (Sect. 6).

Throughout this paper, we adopt the Hubble constant $H_0 = 100\, h\, \mathrm{km\, s^{-1}\, Mpc^{-1}}$ and the deceleration parameter $q_0 = 0.5$.

Send offprint requests to: kurokawa@blackjack.phys.ocha.ac.jp

2. Multifractal analysis

The formal definition of multifractal is not applicable to discrete sets. Hence, for the analysis of the galaxy distribution, several different techniques have been proposed. They are reviewed and compared to each other in Ueda (1995). We employ the "box-counting" method, which appears to be more straightforward than the other existing methods.

Suppose that there are N galaxies in a box of size L. This box is divided into cells of size r. The q-th moment χ_q on the scale r is defined as

$$\chi_q(r) = \sum_{i=1}^{(L/r)^3} \left(\frac{n_i}{N}\right)^q \qquad (q \geq 2). \tag{1}$$

Here n_i is the number of galaxies in the i-th cell ($i = 1, ..., (L/r)^3$). The higher-order moment reflects the structures of the denser regions. We do not study negative-order moments ($q < 0$). If there are vacant cells, they cause divergence of the negative moments.

We plot $\log(\chi_q)$ against $\log(r)$. If the local slope is nearly constant over some range, there is said to be a scaling relation for that range:

$$\chi_q(r) \sim r^{(q-1)D_q} \qquad (r_{min} \leq r \leq r_{max}). \tag{2}$$

Here D_q is the "generalized dimension". Formally, the generalized dimensions are determined by taking the limit $r \to 0$ (Dubrulle & Lachièze-Rey 1994). This is because, only in the limit $r \to 0$, the generalized dimensions correctly yield the important quantities of multifractal, $i.e.$, the Hölder exponent α and the multifractal spectrum $f(\alpha)$. However, in practical analyses of galaxy data, it is impossible to take the limit $r \to 0$.

Furthermore, the distribution of galaxies seems to have different scalings over different ranges of r (Guzzo et al. 1991). Hence almost all the researchers define D_q on finite scales. The D_q values obtained in this way have nearly the same properties as the formal generalized dimensions ($e.g.$, Ueda 1995). We also note that we do not use the quantities α and $f(\alpha)$.

When the distribution is fractal, the scaling relation (2) exists for all the q values. The higher-order generalized dimension characterizes the fractal structure of the denser regions ($e.g.$, Halsey et al. 1986). In a special case of monofractal, all the D_q values are equal to the fractal dimension D_f. This single parameter determines the distribution of the galaxies. If D_f is equal to 3, the distribution is homogeneous. If D_f is less than 3, the galaxies do not uniformly fill the space. For example, a sheet-like distribution yields $D_f = 2$. In a general case of multifractal, D_q is decreasing, $i.e.$, if $q > q'$ then $D_q \leq D_{q'}$. The asymptotic value D_∞ exists in the limit $q \to \infty$.

The two-point correlation function $\xi(r)$ and the power spectrum $p(k)$ provide information about the second-order moment χ_2. Here $k \simeq 2\pi/r$ is the wavenumber. The two-point correlation function $\xi(r)$ is related to the generalized dimension D_2 ($e.g.$, Martínez & Coles 1994):

$$\xi(r) + 1 \sim r^{D_2 - 3}. \quad (3)$$

When $\xi(r)$ is much greater than unity, the above equation is reduced to the usual power-law form of $\xi(r)$:

$$\xi(r) \sim r^{D_2 - 3}. \quad (4)$$

On the other hand, if the spectrum $p(k)$ is expressed as a power law, the exponent is again related to the generalized dimension D_2 ($e.g.$, Guzzo et al. 1991):

$$p(k) \sim k^{-D_2}. \quad (5)$$

From the analyses of $\xi(r) + 1$, Guzzo et al. (1991) obtained $D_2 \simeq 1.2$ at $r \leq 3.5\ h^{-1}$ Mpc and $D_2 \simeq 2.2$ at $3.5 \leq r \leq$ 25–30 h^{-1} Mpc.

However, the second-order moments alone are insufficient to specify the distribution. For example, both the monofractal distribution with $D_f = 2$ and the Gaussian random distribution with $p(k) \sim k^{-2}$ yield $D_2 = 2$. Hence, in order to understand the spatial structures, analyses of the higher-order moments are absolutely required.

3. CfA2 galaxy sample

The CfA2 sample is a flux-limited sample and complete down to $m_{B(0)} = 15.5$. We analyze the data from the survey in the southern sky (Huchra et al. 1999). The survey covers the right ascension range $20^{\rm h} \leq \alpha \leq 4^{\rm h}$ and the declination range $-2.5^\circ \leq \delta \leq 90^\circ$. There are 4392 galaxies in total. We exclude the following areas where the interstellar extinction of our Galaxy is significant: (1) $20^{\rm h} \leq \alpha \leq 21^{\rm h}$, (2) $3^{\rm h} \leq \alpha \leq 4^{\rm h}$, (3) $21^{\rm h} \leq \alpha \leq 2^{\rm h}$ and $b \geq -25^\circ$, (4) $2^{\rm h} \leq \alpha \leq 3^{\rm h}$ and $b \geq -45^\circ$ (Park et al. 1994). Here b is the Galactic latitude.

To obtain the three-dimensional distribution of the galaxies, we derive the comoving coordinate distance d_z from the redshift z:

$$d_z = 6000(1 - 1/\sqrt{1+z})h^{-1}\ {\rm Mpc}. \quad (6)$$

Here we have corrected for the solar motion with respect to the centroid of the Local Group:

$$\Delta v = 300 \sin(l) \cos(b)\ {\rm km\ s^{-1}}, \quad (7)$$

where l is the Galactic longitude. We have also ignored the effect of the peculiar velocities of the individual galaxies. The peculiar velocity is typically 300 km s^{-1} (Davis & Peebles 1983), which corresponds to 3 h^{-1} Mpc. This scale is less than the scales of our interest $\geq 5\ h^{-1}$ Mpc, where a multifractal distribution is found (Sect. 5).

The absolute magnitude $M_{B(0)}$ is obtained from the apparent magnitude $m_{B(0)}$:

$$M_{B(0)} = m_{B(0)} - 5\log[d_z(1+z)] - 25 - Kz, \quad (8)$$

where K is the K-correction factor. We adopt $K = 3$. This value is appropriate for the B-band filter and the median galaxy morphological type Sab (Park et al. 1994).

The multifractal analysis has to be based on a volume-limited sample, where the luminosities of the galaxies are above a certain threshold. An ideal sample has to contain many galaxies as well as to cover a large volume. However, in general, the galaxy number is small at a high luminosity threshold, whereas the volume is small at a low luminosity threshold. We have studied several sets of volume-limited samples. The sample presented here is the one where the scaling law is the most evident (see below).

The magnitude threshold adopted is $M_{B(0)} = -19.42$. The resultant volume-limited sample is illustrated in Fig. 1a. We analyze the largest rectangular box that can be extracted from the volume-limited sample. The box is $42 \times 42 \times 84\ h^{-1}$ Mpc in size, and contains 358 galaxies. The box size L in (1) is set to be $42\ h^{-1}$ Mpc. Here it should be noted that the number of our galaxies is greater than those in the previous multifractal analyses.

To check the generality of the results, we also study the volume-limited sample with the threshold $M_{B(0)} = -20.00$ (Fig. 1b). The box analyzed is $54 \times 54 \times 108\ h^{-1}$ Mpc in size ($L = 54\ h^{-1}$ Mpc), and contains 194 galaxies. Though the galaxy number is small, the box size is greater than the one with $M_{B(0)} = -19.42$. Here we expect that there are not gross differences in the distribution of galaxies at different luminosities (Huchra et al. 1990). For the CfA2 sample, Park et al. (1994) examined the local number density around each galaxy as a function of its absolute magnitude. Both the galaxies with $M_{B(0)} \simeq -19.42$ and those with $M_{B(0)} \simeq -20.00$ exist in all the density regions.

The southern CfA2 sample is known to be dominated by a large flat supercluster, the Pisces-Perseus, which lies at 4000–6000 km s^{-1} in radial velocities (Huchra et al. 1999). This supercluster is partially included in the sample with $M_{B(0)} \leq$

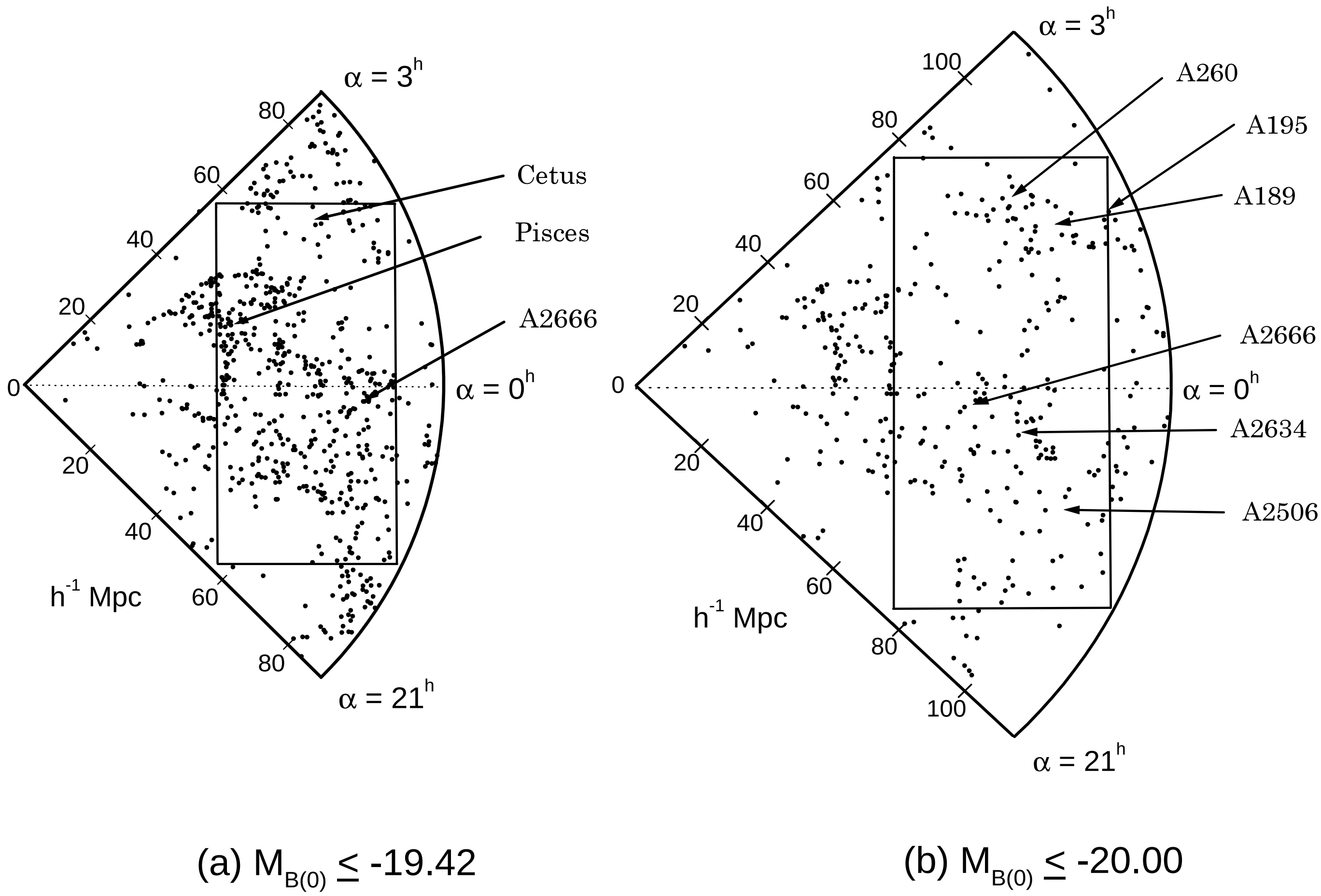

Fig. 1. a Projection of the southern CfA2 galaxies with $M_{B(0)} \leq -19.42$ onto the $\delta = 0°$ plane. The box indicates the region studied in our analysis. We also indicate the positions of the clusters (Huchra et al. 1999). **b** Same as **a**, but with $M_{B(0)} \leq -20.00$.

-19.42. Nevertheless, our analysis is expected to be general. This is because several other clusters are also included in the sample (Fig. 1). Moreover, no remarkable difference is found between the results for the samples with $M_{B(0)} \leq -19.42$ and $M_{B(0)} \leq -20.00$ (Sect. 5). The latter sample does not include the Pisces-Perseus supercluster.

4. Homogeneous and fractal samples

The galaxy sample is composed of a finite number of discrete points. To see the effect of the finiteness and discreteness of the sample, we analyze artificial samples, which are homogeneous ($D_f = 3$) or monofractal ($D_f < 3$).

First, we investigate homogeneous samples. They are generated by distributing 358 or 1500 points uniformly within a box. The shape of the box is the same as that of our galaxy sample. For 100 sets of the homogeneous samples, we compute the mean values and standard deviations of the moments χ_q. The results for $q = 5$ are illustrated in Fig. 2a.

If the distribution is homogeneous and the number of the points is sufficiently large, we have

$$\frac{n_i}{N} \simeq \left(\frac{r}{L}\right)^3 . \quad (9)$$

Hence the moment χ_q is

$$\chi_q(r) \sim r^{3(q-1)} . \quad (10)$$

However, in practice, Eq. (10) is valid only on scales where the number of the cells is much smaller than that of the points (Dubrulle & Lachièze-Rey 1994). If the scale is very small and the number of the cells is very large, every cell contains a single point at most. Even if the scale becomes smaller, the number of the filled cells remains constant. Accordingly, on those small scales, the moment χ_q is simply equal to the value N^{1-q}.

The relation (10) is shown by a dotted line in Fig. 2a. The moments χ_q of the homogeneous samples follow the dotted line down to a certain scale. This scale becomes small as the number of the points is increased, since the mean distance among the points becomes small.

Next, we investigate monofractal samples. We generate "Lévy flight" sets with $D_f = 1.5$ and 2.0 ($e.g.$, Mandelbrot 1982), and extract 358 or 1500 points at random. The moments χ_5 of the fractal samples are illustrated in Fig. 2b ($D_f = 2.0$) and Fig. 2c ($D_f = 1.5$). Dotted lines represent the relations expected for $D_f = 1.5$ and $D_f = 2.0$. The moments for the smaller D_f value lie on the dotted line over a broader range: $r/L \geq 1/11$ for $D_f = 1.5$, $r/L \geq 1/8$ for $D_f = 2.0$, and

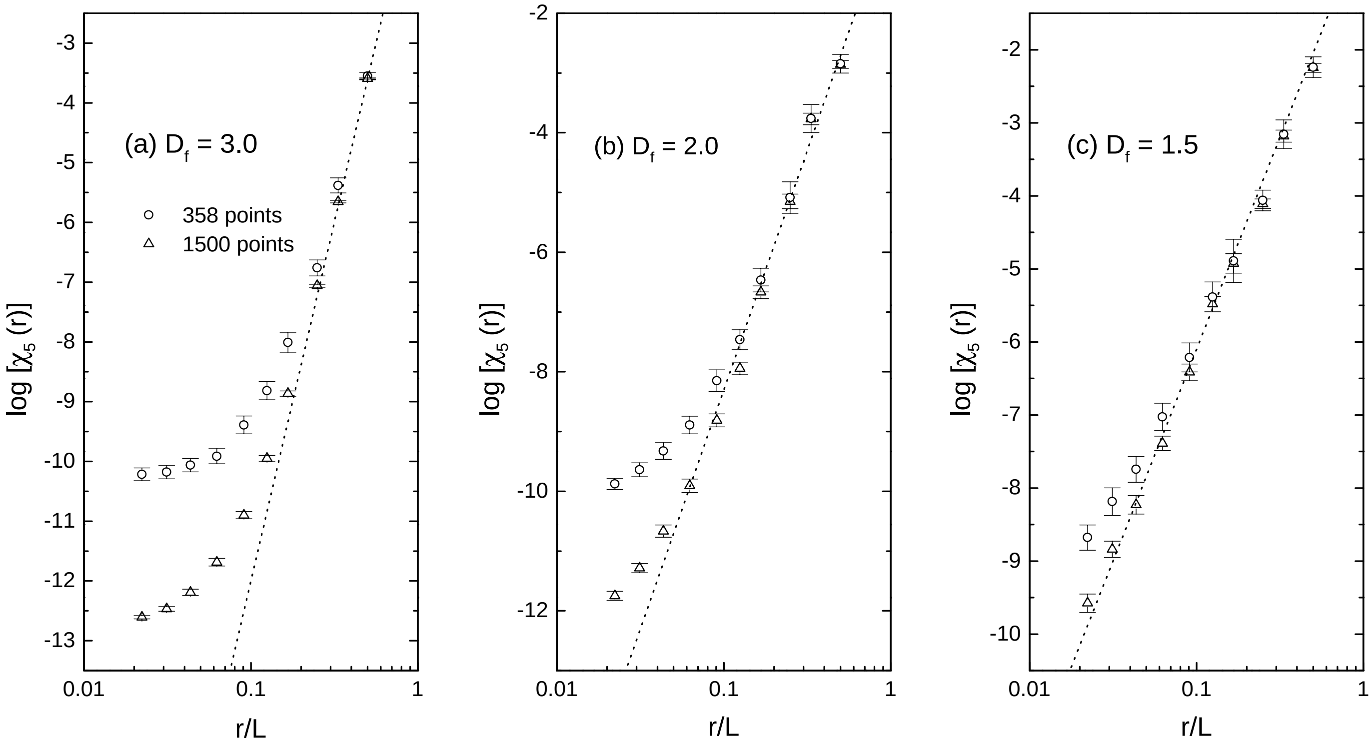

Fig. 2. a The fifth-order moments χ_5 of artificial homogeneous samples with 358 points (open circles) and 1500 points (open triangles). The dotted line represents the relation expected for a homogeneous distribution. **b** Same as **a**, but for a Lévy fractal sample with $D_f = 2.0$. **c** Same as **a**, but for a Lévy fractal sample with $D_f = 1.5$.

$r/L \geq 1/4$ for $D_f = 3.0$, in the case of 358 points. This is because a fractal structure has local clusters of points. The effective mean distance among the points is smaller in a fractal set with a smaller D_f value.

5. Results

The moments χ_q of our galaxy sample with $M_{B(0)} \leq -19.42$ are computed for $q = 2$–9 and for $r = 1$–21 h^{-1} Mpc ($r/L = 1/45$–1/2). The results for $q = 2$, 5, and 9 are illustrated in the panels of Fig. 3 (filled circles). For reference, we also plot the moments of the homogeneous samples with 358 points (open circles). The scales r in units of h^{-1} Mpc are indicated on the upper axes. The vertical bars on the galaxy moments represent the 1σ statistical errors evaluated with the "bootstrap resampling" method (Efron 1982; Barrow et al. 1984).

For every q and every r, the moment χ_q of our galaxy sample is clearly different from the moment of the homogeneous samples. Thus the galaxy distribution has certain structures. We apply the least-squares fit to the galaxy moments on the five scales 5, 7, 11, 14, and 21 h^{-1} Mpc ($r/L =$ 1/8, 1/6, 1/4, 1/3, and 1/2). This spacing is roughly 0.5 in logarithms. The results are shown by solid lines in Fig. 3. From 5 to 21 h^{-1} Mpc, the galaxy moments lie on the solid lines. This means that there is the scaling relation (2). The same results have been obtained for the other moments, which are not shown in Fig. 3. We have also found the scaling relation from 7 to 27 h^{-1} Mpc in the sample with $M_{B(0)} \leq -20.00$.

Below the scale 5 h^{-1} Mpc in Fig. 3, the galaxy moments χ_q do not follow the scaling relation. Those moments suffer from the finiteness of the galaxy number. The scale where the finiteness becomes important is smaller in the galaxy sample than in the homogeneous samples. This is because the galaxy distribution has spatial structures. The scaling regime of our galaxy sample is rather comparable to the scaling regime of the monofractal samples studied in Sect. 4.

The generalized dimensions D_q are derived from the scaling exponents, $i.e.$, the slopes of the solid lines in Fig. 3. The results for $M_{B(0)} \leq -19.42$ (filled circles) and $M_{B(0)} \leq -20.00$ (open squares) are shown as a function of q in Fig. 4. The vertical bars on the data points represent the 1σ uncertainties associated with the least-squares fit, which incorporate the statistical errors of the individual moments. Within the 1σ uncertainties, the results for the two samples are consistent. The D_q value decreases as q is increased. Therefore, over the scale and order ranges considered here, the galaxy distribution satisfies the requirement for the multifractal distribution.

We have presented only the galaxy moments χ_q with $q \leq 9$. The statistical errors of the higher-order moments are quite large. With an increase of q above 10, the generalized dimension D_q seems to converge to ~ 1.3 and ~ 1.5, respectively, in the samples with $M_{B(0)} \leq -19.42$ and $M_{B(0)} \leq -20.00$. Their scaling ranges seem to be the same as those for $q \leq 9$. Thus the asymptotic value D_∞ seems to be at around 1.4. This result has to be confirmed in future with a larger galaxy sample.

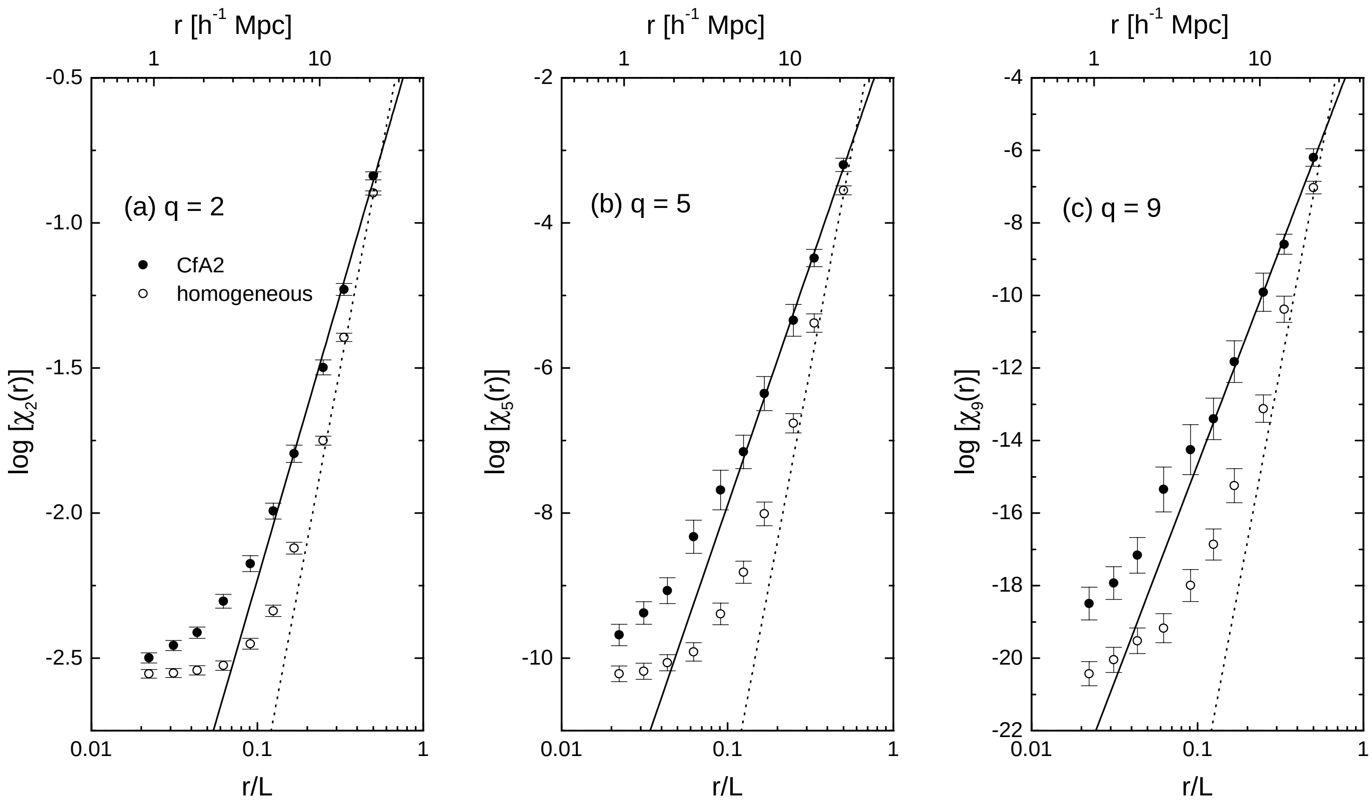

Fig. 3. a The second-order moments χ_2 of the galaxy sample (filled circles) and those of the artificial homogeneous samples (open circles). The solid line is the result of the least-squares fit. The dotted line represents the relation expected for a homogeneous distribution. **b** Same as **a**, but for the fifth-order moments χ_5. **c** Same as **a** but for the ninth-order moments χ_9.

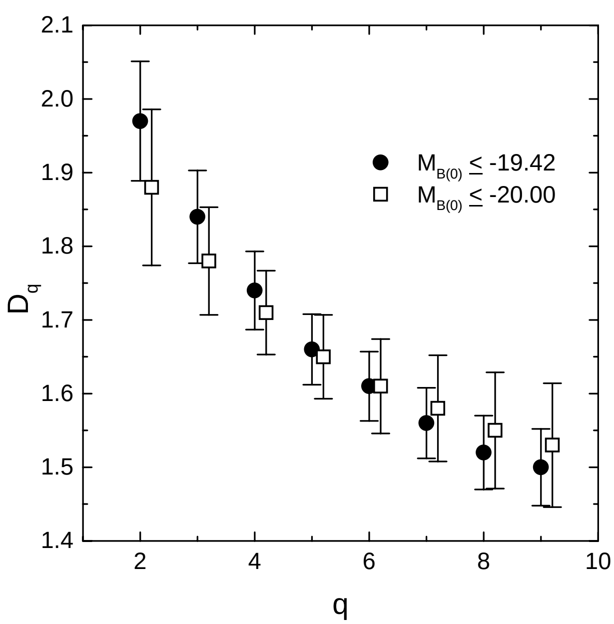

Fig. 4. The generalized dimension D_q for the galaxy samples with $M_{B(0)} \leq -19.42$ (filled circles) and with $M_{B(0)} \leq -20.00$ (open squares).

6. Discussion

The scales where we have found the multifractal law are from 5–7 to 21–27 h^{-1} Mpc. On these scales, the existence of scalings has been already noticed. Guzzo et al. (1991) examined $\xi(r) + 1$ with the data from the Perseus-Pisces and CfA surveys. Between 3.5 and 25–30 h^{-1} Mpc, the function $\xi(r) + 1$ has a power-law form (3) with $D_2 \simeq 2.2$.[1] Lin et al. (1996) examined the spectrum measured from the Las Campanas Redshift survey. Between 5 and 30 h^{-1} Mpc, the spectrum has a power-law form (5) with $D_2 \simeq 1.8$. These D_2 values are consistent with ours. Similar features were also observed in the spectra from the IRAS-QDOT and APM surveys (Peacock 1997; Guzzo 1997). Finally, Domínguez-Tenreiro et al. (1994) made multifractal analyses on the CfA1 survey with the methods "correlation integral" and "density reconstruction" (consult Ueda 1995 for these techniques). They found multifractal scalings up to 20–30 h^{-1} Mpc.

With the results of D_2 alone, one might consider that the observed scaling originates simply in a Gaussian random field with $p(k) \sim k^{-2}$ (Sect. 2). Nevertheless, our analysis of the

[1] The behavior of $\xi(r) + 1$ in the Perseus-Pisces sample is similar to the behavior in the (northern) CfA sample. This result supports the generality of our result on the southern CfA2 sample, since the Perseus-Pisces and southern CfA2 surveys cover nearly the same volumes.

higher-order moments reveals the existence of the spatial structures.

The D_2 value for our CfA2 samples is about 2. This value is obtained if the galaxies are in planar structures. With increasing the order q from 2 to 9, the D_q value decreases toward ~ 1. Since the higher-order moments give more weight to the dense regions, those D_q values are obtained if there are filament-like dense regions within the planar structures. Galaxies are known to be distributed roughly on the walls of spherical voids ($e.g.$, Geller & Huchra 1989). From the topology of isodensity contours of the CfA2 galaxies, Vogeley et al. (1994) claimed that the distribution is like "walls with holes" or a "filamentary net". Our present result corresponds to the quantitative description of those structures.

There are several processes that can explain the presence of the above structures. The first possibility is the gravitational instability, where the structures evolved from the primordial random fluctuations (see Jenkins et al. 1998 for the most recent N-body simulation). The second possibility is the presence of topological defects such as "domain walls" arising from a phase transition in the early universe (Vilenkin 1985). The last possibility is the explosions of the first-generation supernovae, which might have swept the ambient gas and generated a network of thin shells (Ikeuchi 1981; Ostriker & Cowie 1981). These models can reproduce, at least qualitatively, the planar structures with filamentary dense regions. To specify the most plausible model, multifractal analyses of the model predictions are important.

The observed multifractal scaling is unlikely to extend to the smaller scales $r \ll$ 5–7 h^{-1} Mpc. The value $D_2 \simeq 2$ obtained in our analysis is different from the value $D_2 \simeq 1.2$ obtained by Guzzo et al. (1991) for $r \leq 3.5$ h^{-1} Mpc. The galaxy moments on those small scales are likely to reflect the internal structure of galaxy clusters, which are the predominant entities on scales less than a few Mpc. In fact, $D_2 \simeq 1.2$ is well reproduced by a distribution of density singularities with a certain profile (Murante et al. 1997).

7. Concluding remarks

The scaling properties of the galaxy number density have been explored through the multifractal analysis of the CfA2 data. The box-counting method has been employed (Sect. 2). With the luminosity thresholds $M_{B(0)} = -19.42$ and -20.00, we have constructed two complete samples. The one is $42 \times 42 \times 84$ h^{-1} Mpc in size and contains 358 galaxies. The other is $54 \times 54 \times 108$ h^{-1} Mpc in size and contains 194 galaxies (Sect. 3). The confidence of our analyses has been ensured with artificial samples (Sect. 4). On scales from 5–7 to 21–27 h^{-1} Mpc, we have found multifractal scalings (Sect. 5). The measured generalized dimensions D_q are consistent with the picture that galaxies lie in planar structures which have filamentary dense regions (Sect. 6).

Because of the limitation of the volume size and galaxy number of the CfA2 sample, we have been unable to determine the entire scale range of the multifractal distribution. If the entire range were determined, it could put constraints on scenarios for the formation of the multifractal structures. The analysis of Guzzo et al. (1991) with $\xi(r) + 1$ implies that the second-order moment scales as $D_2 \simeq 2.2$ up to 30 h^{-1} Mpc (but see also Sylos-Labini et al. 1998 for the argument for the never-ending scaling of $D_2 \simeq 2$). However, with the D_2 value alone, it is uncertain whether or not the spatial structures exist. Scaling analyses of the higher-order moments are required. We expect that future redshift surveys would provide galaxy data of greater volumes. Of equal importance is to develop a new technique and to study the scaling properties of the existing data over wider ranges.

Acknowledgements. The authors are grateful to J. P. Huchra for providing us with permission to use the CfA2 data in advance of the publication, and to M. Lachièze-Rey for useful comments. H. M. thanks H. Kubotani, M. Noda, Y. Taniguchi, M. Umemura, and A. Yoshisato for interesting discussion.

References

Barrow J.D., Bhavsar S.P., Sonoda D.H., 1984, MNRAS 210, 19P
Coleman P.H., Pietronero L., 1992, Phys. Rep. 213, 311
Davis M., Peebles P.J.E., 1983, ApJ 267, 465
Domínguez-Tenreiro R., Gómez-Flechoso M.A., Martínez V.J., 1994, ApJ 424, 42
Dubrulle B., Lachièze-Rey M., 1994, A&A 289, 667
Efron B., 1982, The Jackknife, the Bootstrap, and Other Resampling Plans. S.I.A.M, Philadelphia
Geller M.J., Huchra J.P., 1989, Sci 246, 897
Guzzo L., 1997, New Astronomy 2, 517
Guzzo L., Iovino A., Chincarini G., Giovanelli R., Haynes M.P., 1991, ApJ 382, L5
Halsey T.C., Jensen M.H., Kadanoff L.P., Procaccia I., Shraiman B.I., 1986, Phys. Rev. A 33, 1141
Huchra J.P., Geller M.J., de Lapparent V., Corwin H.G., 1990, ApJS 72, 433
Huchra J.P., Vogeley M.S., Geller M.J., 1999, ApJS, in press (CfA Preprint 4486)
Ikeuchi S., 1981, PASJ 33, 211
Jenkins A., Frenk C.S., Pearce F.R., et al., 1998, ApJ 499, 20
Jensen M.H., Kadanoff L.P., Libchaber A., Procaccia I., Stavans J., 1985, Phys. Rev. Lett. 55, 2798
Jones B.J.T., Martínez V.J., Saar E., Einasto J., 1988, ApJ 332, L1
Lin H., Kirshner R.P., Shectman S.A., et al., 1996, ApJ 471, 617
Mandelbrot B.B., 1982, The Fractal Geometry of Nature. Freeman, San Francisco
Martínez V.J., Coles P., 1994, ApJ 437, 550
Murante G., Provenzale A., Spiegel E.A., Thieberger R., 1997, MNRAS 291, 585
Ostriker J.P., Cowie L.L., 1981, ApJ 243, L127
Parisi G., Frisch U., 1985, On the singularity structure of fully developed turbulence. In: Ghil M., Benzi R., Parisi G. (eds.) Turbulence and Predictability in Geophysical Fluid Dynamics. North-Holland, Amsterdam, p. 84
Park C., Vogeley M.S., Geller M.J., Huchra J.P., 1994, ApJ 431, 569
Peacock J.A., 1997, MNRAS 284, 885
Sylos-Labini F., Montuori M., Pietronero L., 1998, Phys. Rep. 293, 61
Ueda H., 1995, PASJ 47, 389
Vilenkin A., 1985, Phys. Rep. 121, 262
Vogeley M.S., Park C., Geller M.J., Huchra J.P., Gott III J.R., 1994, ApJ 420, 525